Nigerian Journal of Science and Environment 2025 Volume 23 (2) 177 – 187 ISSN: 3043 – 4440
https://doi.org/10.61448/njse2322514

DETERMINATION OF THE SAFETY OF BURIED PIPELINES IN OLOGBO, EDO STATE USING SCHLUMBERGER ELECTRICAL RESISTIVITY METHOD

[1]Tamunosiki, D. and [2]Chiemeke, C.C

[1]Department of Physics, Federal University Otuoke, P.M.B 126 Bayelsa State.
[2]Department of Physics, Federal University Otuoke, P.M.B 126 Bayelsa State.

[*]Corresponding Author's Email: dieokumat@fuotuoke.edu.ng; (Telephone: +2348034622954)

Abstract

Electrical surveys are usually employed to determine the subsurface resistivity distribution by making measurements on the ground surface. From these measurements, the true resistivity of the subsurface can be estimated. The ground resistivity is related to various geological parameters such as the mineral and fluid content, porosity and degree of water saturation in the rock. In this article, Electrical resistivity measurement was carried out at the ELPS CS1site at Ologbo Edo State. The tests were conducted at six points on the project site based on the predetermined AB/2 spacing and Mn/2 spacing for Schlumberger method. The K factor was used to convert the resistance in Ω measured in the field to apparent resistivity in Ωm. The resulting apparent resistivity was subjected to an inversion process that turned the apparent resistivity to the true resistivity of the subsurface. The 1D resistivity models shows values are within the range of 55.2 Ωm to 9805 Ωm, within an investigated depths of 10 m while the 3D electrical resistivity contour for both the surface and 5 m depth, depicts the distribution of electrical resistivity within the investigated site. It shows area of low and high electrical resistivity values. 1D and 3D electrical resistivity models, gave a clear indication that majority of the determined electrical resistivity values from the surface, down to a depth of 5 m, are greater than5 Ωm.

Key Words: Electrical Resistivity, K Factor. Inversion, Porosity

Introduction

The purpose of electrical surveys is to determine the subsurface resistivity distribution by making measurements on the ground surface. From these measurements, the true resistivity of the subsurface can be estimated. The ground resistivity is related to various geological parameters such as the mineral and fluid content, porosity and degree of water saturation in the rock; Obrike *et al*. (2007). Electrical resistivity surveys have been used for many decades in hydro geological, mining and geotechnical investigations. More recently, it has been used for environmental surveys; Short and Stauble, (1967). Two method of data collection are majorly used for data acquisition in electrical resistivity survey, these are Schlumberger method popularly known as VES (Vertical Electrical Sounding), which involve keeping the potential electrodes constant, while expanding the current electrode. The second method is the Wenner Method, which involve maintaining equal distance between the four electrodes at the point of each measurement.

This study aims to evaluate the subsurface soil resistivity at a pipeline test site in Ologbo, Edo State, using the Schlumberger electrical resistivity method, in order to assess the potential for corrosion and the consequent need (or lack thereof) for cathodic protection of buried pipelines. This study aims to evaluate the subsurface soil resistivity at a pipeline test site in Ologbo, Edo State, using the Schlumberger electrical resistivity method, in order to assess the potential for corrosion and the consequent need (or lack thereof) for cathodic protection of buried pipelines. This will be achieved by identifying and establishing appropriate geophysical test points, processing, analyzing and interpretation of data to derive true resistivity and to interpret the geoelectrical data with respect to corrosion potential and site suitability.

General geology of the Area of study: Cretaceous to Tertiary Sedimentary formations occupies over eighty percent of Edo State. Some cretaceous sediments of Anambra Basin and tertiary sediments of Niger Delta sequences are found in the study area. These formations contain clay deposits. The Azagba-Ogwashi Formation has been often spelt as Ogwashi-Asaba Formation consists of clays, sands and grits and seams of lignite alternating with gritty clays. It grades upwards into the Benin Formation. The Ogwashi Asaba Formation is exposed in stream channels at the northern parts of the Benin Region, west of Ekiadolor-Iwu and 4 km east of Utekon and north of Azalla (Reyment, 1965). The Benin Formation is assigned to the Oligocene-Pleistocene period in the continent of Africa and to the Oligocene-Pleistocene to recent at the sub oceanic; Short and Stauble (1967). The formation is characterized by top reddish to reddish brown lateritic massive indurate clay and sand. This is often marked with reticulate mud racks. This cap the underlying more friable pinkish-yellowish white often gravelly-pebble sands clayey soils, sands and clay (Akujieze, 2004). The sedimentary sequences are poorly bedded with discontinuous clay horizons at various depths.

It is estimated to be about 800m thick under Benin City and about 1,830 m near the seashore sections of the formation. They are exposed at various erosion sites, sand quarry sites, and road cuttings. Regionally, the Imo Shale, which sits on top of the Nsukka Formation, reveals a shallow marine shelf environment with preserved foreshore and shoreface sands (Petters and Ekweozor (1981) and Obirike (2012). It also contains black shales, blue-grey clays, and marl with interspersed calcareous sandstone, marl, and limestone (Onyekuru *et al*. 2018). According to Obirike et al. (2007) and Onyekuru *et al*. (2018), regression persisted throughout the Eocene and culminated in the formation of Lower and Middle Eocene deposits, which include the clastic Ameki and Nanka Formations. The transition back to regressive conditions is marked by the progradational Nanka Formation. In the northern parts of the Niger Delta, the Agbada Formation represents the subsurface deposits of the prograding shoreface and river plain, while the Akata Formation refers to the marine Imo Shale counterpart. The Oligocene-Recent Ogwashi-Asaba and Benin Formations dominate the area's uppermost lithostratigraphic units of the stratigraphic succession (Nwajide (2005) and Okoye and Obi (2011). In the Miocene period, the Niger Delta sediments accumulate and prograde seawards. As a result, the sea level is lowered during the Pleistocene. The Niger River cut wide valleys through its own delta. These troughs are being filled today as the sea level gradually rises (Okoye and Obi 2011).

Materials and Method

Electrical resistivity measurement was carried out at the ELPS CS1 site at Ologbo Edo State. The Electrical resistivity tests were conducted at six points. The map of the survey area depicting the points of data acquisition for Electrical resistivity is shown in figure 1 while the coordinates of the points are shown in Table 1. Electrical resistivity measurement is majorly carried out to determine the distribution of electrical resistivity of the soil at the surface and within the subsurface. This is majorly achieved by injecting current into the ground through the current electrodes and measuring the resulting potential through the potential electrodes. This was used to determine the electrical property of the soil necessary for site characterization.

Table 1: Electrical Resistivity Test Location Points and Coordinates

Electrical Points	Coordinates	
	Easting	Northing
ERT1 (RT1)	675749.568	799073.125
ERT2 (RT2)	675688.664	799094.667
ERT3 (RT3)	675925.433	799071.792
ERT4 (RT4)	675632.360	799062.007
ERT5 (RT5)	675630.753	799100.500
ERT6 (RT6)	675781.913	799122.206

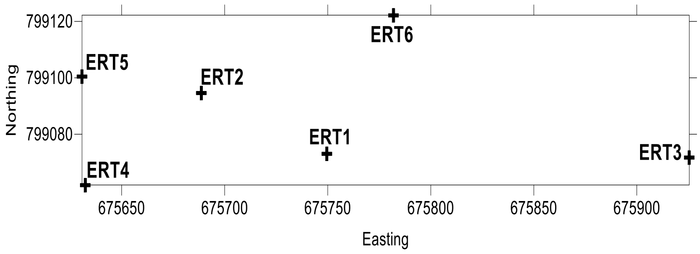

Figure 1: Work Layout showing the points where Electrical Resistivity test were carried out.

Data Acquisition: The electrical resistivity data were acquired in various locations. The data acquisition for resistivity survey started with inserting four electrodes into the ground base on the predetermined AB/2 spacing and Mn/2 spacing for Schlumberger method. The two outer electrodes are current electrodes, while the two inner electrodes are the potential electrodes. The reels of cables were connected to their corresponding electrodes, which was also connected to the SAS 1000 Terameter. The SAS 1000 Terameter was powered up after connecting it to a 12V battery. After the initial booting and settings protocols, measurement was initiated, the resistance in Ω of the subsurface was measured, and recorded. The distance between the current electrodes were increased, while keeping the distance between the potential electrodes constant, the measurement was repeated until the desired spread length was achieved for the Schlumberger array configuration employed.

Data Processing: The recorded resistance values of the subsurface in Ω were entered into a spread sheet. The K factor was used to convert the resistance in Ω measured in the field to apparent resistivity in Ωm (See Tables 1-6). The resulting apparent resistivity was subjected to an inversion process that turned the apparent resistivity to the true resistivity of the subsurface. The true resistivity values were plotted on a log log graph, with a table showing the resistivity of each layer, the depth and thickness of each layer (see figures 1-6). 3D contour maps of the 1D resistivity values at the surface and at a depth of 5m were produced (see Figures 7-8 and Table 7), to enhance the visualization of the distribution of soil resistivity.

Results

The 1D resistivity models of figures 1 to 6, gave indications that electrical resistivity values of the investigated sites, are within the range of 55.2 Ωm to 9805Ωm, within an investigated depths of 10m generally, the 1D resistivity models showed evidence of starting with high electrical resistivity values that decrease progressively to a particular depth and increase again. The 3D electrical resistivity contour shown in figure 7 and 8, for both the surface and 5m depth, depicts the distribution of electrical resistivity within the investigated site. It shows area of low and high electrical resistivity values. The values of the registered electrical resistivity, couple with the plot and shape of the 1D and 3D electrical resistivity models, gave a clear indication that majority of the determined electrical resistivity values from the surface, down to a depth of 5m, are greater than 5 Ωm.

Table 2: ELPS CS1 ERT1 (RT1), VES, Current Electrode spacing, Potential Electrode Spacing, Measured Resistance, and calculated Apparent Resistivity(Ωm)for Schlumberger Electrical Resistivity Method.

Depth (m)	AB/2 (m)	Mn/2 (m)	Resistance (Ω)	Apparent Resistivity(Ωm)
0.3	1	0.5	726.3	2282.657143
0.4	1.5	0.5	217.73	1539.662143
0.6	2	0.5	107.81	1355.325714
1.0	3	0.5	43.182	1221.433714
1.5	5	0.5	12.063	947.8071429
2.0	7	1.5	5.1062	262.1182667
3.0	10	1.5	6.0211	630.7819048
5.0	15	3	6.963	820.6392857
6.0	20	3	4.6114	966.1980952
8.0	25	3	3.3097	1083.532738
9.0	30	3	2.6633	1255.555714
10	35	3	2.0862	1338.645000

https://doi.org/10.61448/njse2322514

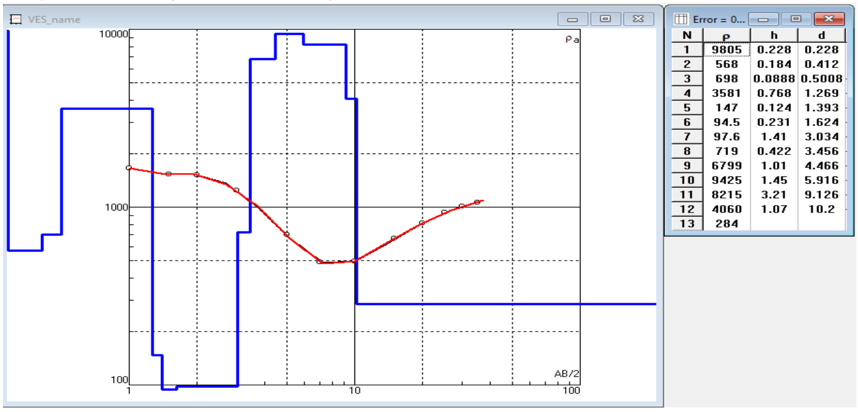

Figure 2: ELPS CS1 ERT 1, VES, Schlumberger 1D Electrical Resistivity Model for Resistivityρ, Layer Thickness$h$, and Depth d

Table 3: ELPS CS1 ERT2 (RT2), VES, Current Electrode spacing, Potential Electrode Spacing, Measured Resistance, and calculated Apparent Resistivity(Ωm) for Schlumberger Electrical Resistivity Method.

epth (m)	**B/2 (m)**	**In/2 (m)**	**esistance (Ω)**	**pparent Resistivity(Ωm)**
3		5	29.22	20.4057143
4	5	5	)4.25	37.1964286
6		5	7.826	75.5268571
0		5	5.943	50.9591429
5		5	4565	35.8678571
0		5	1018	10.5590667
0	)	5	4013	55.8504762
0	5		0298	28.5121429
0	)		4458	31.5009524
0	5		4776	11.1190476
0	)		0076	46.4400000
)	5		6957	)88.074167

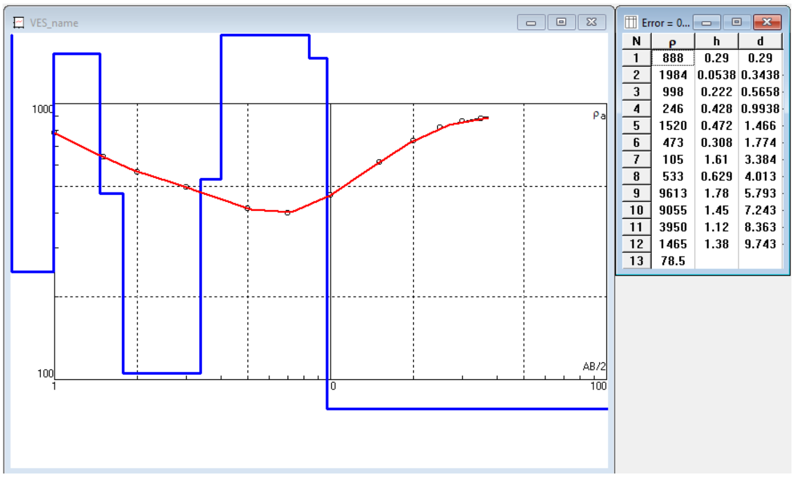

Figure 3: ELPS CS1 ERT 2, VES, Schlumberger 1D Electrical Resistivity Model for Resistivityρ, Layer Thickness$h$, and Depth d

Nigerian Journal of Science and Environment 2025 Volume 23 (2) 177 – 187 ISSN: 3043 – 4440
https://doi.org/10.61448/njse2322514

Table 4: ELPS CS1 ERT3 (RT3), VES, Current Electrode spacing, Potential Electrode Spacing, Measured Resistance, and calculated Apparent Resistivity(Ωm) for Schlumberger Electrical Resistivity Method.

Depth (m)	AB/2 (m)	Mn/2 (m)	Resistance (Ω)	Apparent Resistivity(Ωm)
0.3	1	0.5	242.73	762.8657143
0.4	1.5	0.5	89.658	634.0101429
0.6	2	0.5	48.774	613.1588571
1.0	3	0.5	22.065	624.1242857
1.5	5	0.5	9.8512	774.0228571
2.0	7	1.5	13.399	687.8153333
3.0	10	1.5	5.6937	596.4828571
5.0	15	3	7.8562	925.9092857
6.0	20	3	3.7083	776.9771429
8.0	25	3	3.3231	1087.919643
9.0	30	3	2.1292	1003.765714
10	35	3	1.6239	1042.002500

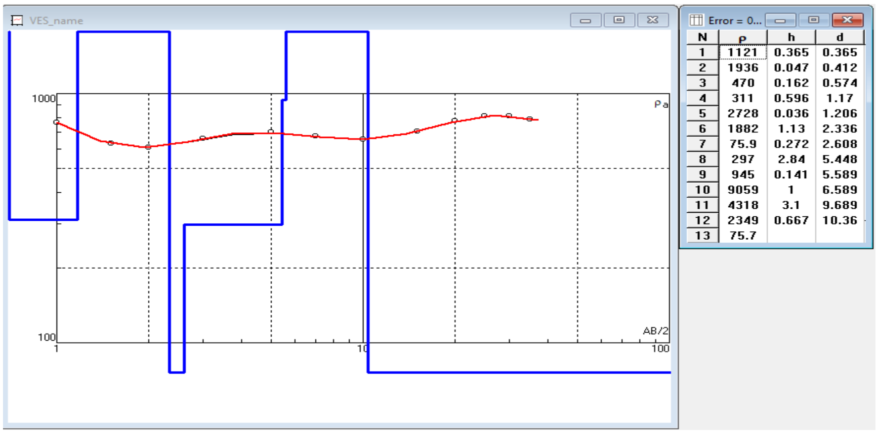

Figure 4: ELPS CS1 ERT 3, VES, Schlumberger 1D Electrical Resistivity Model for Resistivityρ, Layer Thickness$h$, and Depth d

Table 5: ELPS CS1 ERT4 (RT4), VES, Current Electrode spacing, Potential Electrode Spacing, Measured Resistance, and calculated Apparent Resistivity(Ωm) for Schlumberger Electrical Resistivity Method.

Depth (m)	AB/2 (m)	Mn/2 (m)	Resistance (Ω)	Apparent Resistivity(Ωm)
0.3	1	0.5	344.73	1083.437143
0.4	1.5	0.5	135.07	955.1378571
0.6	2	0.5	39.913	501.7634286
1.0	3	0.5	14.297	404.4008571
1.5	5	0.5	7.731	607.4357143
2.0	7	1.5	11.557	593.2593333
3.0	10	1.5	5.6415	591.0142857
5.0	15	3	7.0189	827.2275000
6.0	20	3	4.5982	963.4323810
8.0	25	3	3.7749	1235.830357
9.0	30	3	3.7445	1765.264286

10	35	3	2.5656	1646.260000

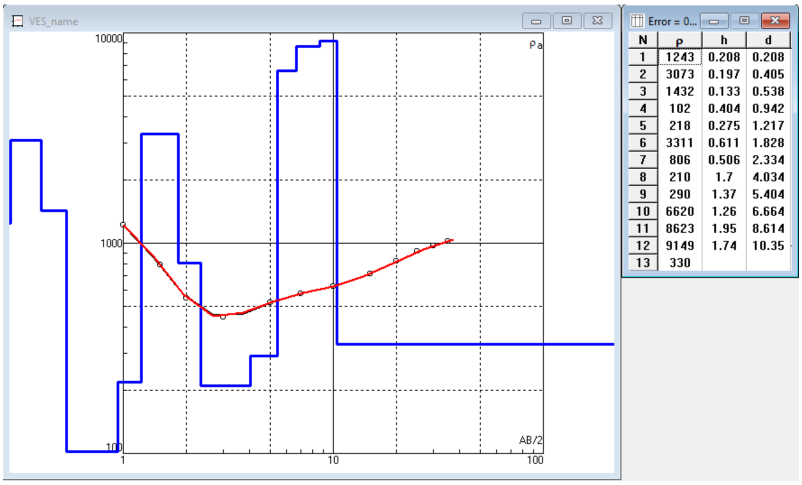

Figure 5: ELPS CS1 ERT 4, VES**,** Schlumberger 1D Electrical Resistivity Model for Resistivity ρ, Layer Thickness h, Depth d

Table 6: ELPS CS1 ERT5 (RT5), VES, Current Electrode spacing, Potential Electrode Spacing, Measured Resistance, and calculated Apparent Resistivity(Ωm) for Schlumberger Electrical Resistivity Method.

Depth (m)	**AB/2 (m)**	**Mn/2 (m)**	**Resistance (Ω)**	**Apparent Resistivity(Ωm)**
0.3	1	0.5	320.35	1006.814286
0.4	1.5	0.5	113.46	802.3242857
0.6	2	0.5	68.455	860.5771429
1.0	3	0.5	32.148	909.3291429
1.5	5	0.5	11.308	888.4857143
2.0	7	1.5	20.600	1057.466667
3.0	10	1.5	10.801	1131.533333
5.0	15	3	9.8225	1157.651786
6.0	20	3	5.6895	1192.085714
8.0	25	3	3.9520	1293.809524
9.0	30	3	2.8655	1350.878571
10	35	3	2.5603	1642.859167

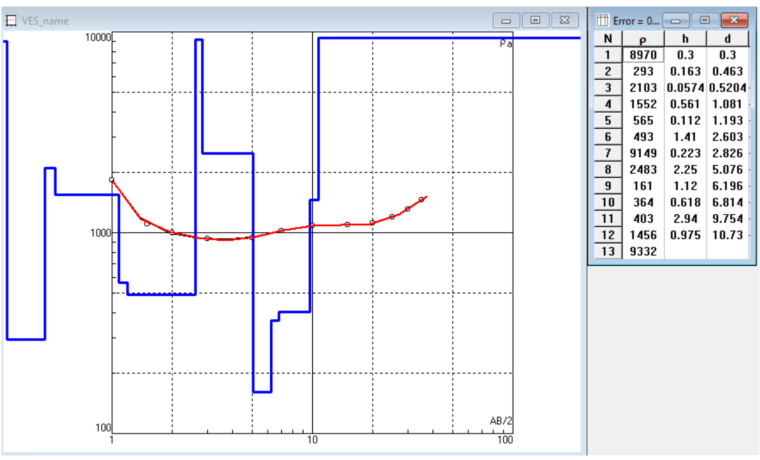

Figure 6: ELPS CS1 ERT 5, VES, Schlumberger 1D Electrical Resistivity Model for Resistivity ρ, Layer Thickness h, Depth d

Nigerian Journal of Science and Environment 2025 Volume 23 (2) 177 – 187 ISSN: 3043 – 4440
https://doi.org/10.61448/njse2322514

Table 7: ELPS CS1 ERT6 (RT6), VES, Current Electrode spacing, Potential Electrode Spacing, Measured Resistance, and calculated Apparent Resistivity(Ωm) for Schlumberger Electrical Resistivity Method.

Depth (m)	AB/2 (m)	Mn/2 (m)	Resistance (Ω)	Apparent Resistivity($\boldsymbol{\Omega m}$)
0.3	1	0.5	156.92	493.1771429
0.4	1.5	0.5	63.01	445.5707143
0.6	2	0.5	16.957	213.1737143
1.0	3	0.5	7.4112	209.6310857
1.5	5	0.5	4.498	353.4142857
2.0	7	1.5	8.6148	442.2264000
3.0	10	1.5	4.4091	461.9057143
5.0	15	3	6.4152	756.0771429
6.0	20	3	4.5619	955.8266667
8.0	25	3	3.3705	1103.437500
9.0	30	3	2.745	1294.071429
10	35	3	2.304	1478.400000

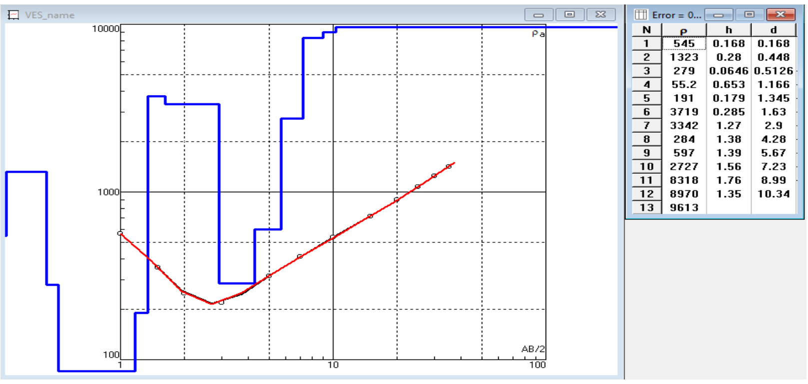

Figure 7: ELPS CS1 ERT 6, VES, Schlumberger 1D Electrical Resistivity Model for Resistivityρ, Layer Thickness$h$, and Depth d

Table 8: Coordinates of 3D contour of Electrical Resistivity distribution at the surface

Electrical Points	Coordinates		Electrical Resistivity Values in($\boldsymbol{\Omega m}$)
	Easting	Northing	
ERT1 (RT1)	675749.568	799073.125	9805
ERT2 (RT2)	675688.664	799094.667	888
ERT3 (RT3)	675925.433	799071.792	1121
ERT4 (RT4)	675632.360	799062.007	1243
ERT5 (RT5)	675630.753	799100.500	8970
ERT6 (RT6)	675781.913	799122.206	545

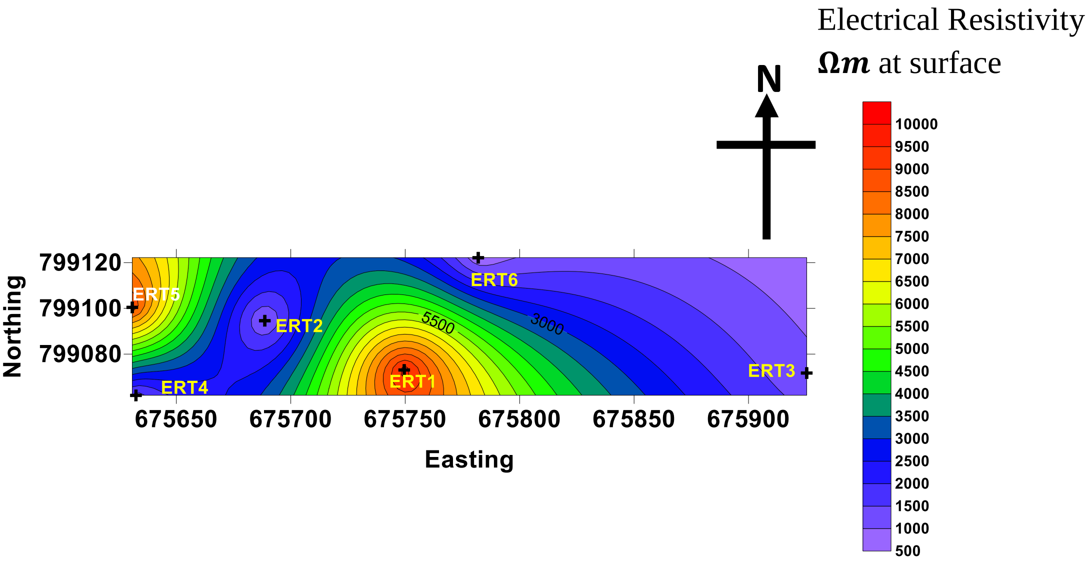

Figure 8: 3D Contour of electrical resistivity distribution within the test site at the surface

Table 9: Coordinates of 3D contour of Electrical Resistivity distribution at 5 m depth

Electrical Points	**Coordinates**		Electrical Resistivity Values in(Ωm)
	Easting	**Northing**	
ERT1 (RT1)	675749.568	799073.125	9425
ERT2 (RT2)	675688.664	799094.667	9613
ERT3 (RT3)	675925.433	799071.792	297
ERT4 (RT4)	675632.360	799062.007	290
ERT5 (RT5)	675630.753	799100.500	2483
ERT6 (RT6)	675781.913	799122.206	597

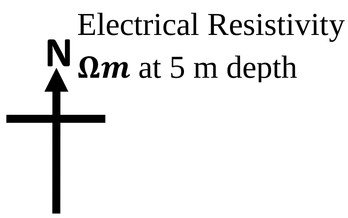

Nigerian Journal of Science and Environment 2025 Volume 23 (2) 177 – 187 ISSN: 3043 – 4440
https://doi.org/10.61448/njse2322514

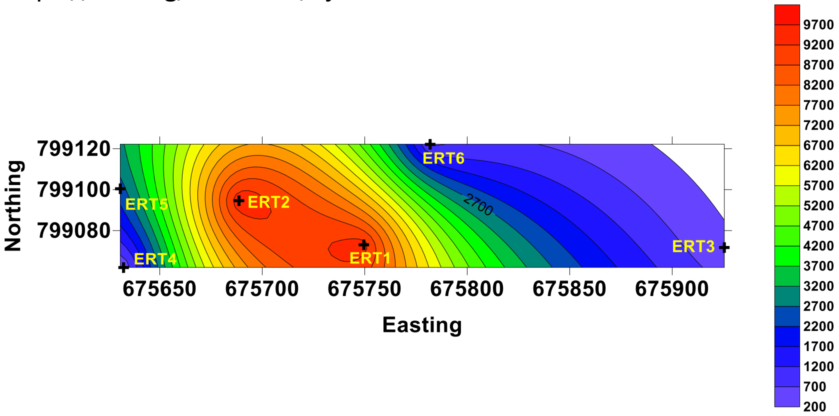

Figure 9: 3D Contour of electrical resistivity distribution within the test site at 5 m depth.

Discussion

The electrical resistivity results obtained from this study provide valuable insights into the subsurface. .conditions at the ELPS CS1 site in Ologbo, Edo State. The findings are supported by both 1D resistivity models (Figures 2–7) and 3D resistivity distribution maps (Figures 8–9), which collectively highlight the spatial and vertical variations in soil resistivity and their implications for pipeline safety. The vertical stratification observed in Figures 2-7 aligns with contemporary characterizations of tropical lateritic soils in the Benin Formation, where near-surface induration creates high-resistivity layers (Ezeh et al., 2023), transitioning to clay-rich intermediate zones.

Resistivity Distribution and Geological Implications - The 1D resistivity models (Figures 2–7) reveal a consistent trend of high resistivity values (>1000 Ωm) in the near-surface layers, followed by a decrease at intermediate depths (1–3 m), and a subsequent increase in deeper layers (>5 m). This stratification aligns with the known geology of the Benin Formation (Akujieze, 2004), where lateritic topsoil transitions into clay-rich intermediate layers and finally into more consolidated sandy deposits. Notably, the resistivity range of 55.2–9805 Ωm across all test points significantly exceeds the 5 Ωm threshold for corrosion risk (NACE SP0169), indicating excellent natural protection for buried pipelines.

The 3D resistivity contours (Figures 8–9) further illustrate the spatial variability of resistivity across the site. Figure 8 (surface distribution) shows higher resistivity values (>1000 Ωm) concentrated in the northwestern region, particularly at ERT1 (9805 Ωm) and ERT5 (8970 Ωm). In contrast, lower resistivity zones (~500–1000 Ωm) are observed in the northeastern sector (e.g., ERT6 at 545 Ωm). At 5 m depth (Figure 9), resistivity remains high in most areas, though localized lows (~290 Ωm) appear at ERT3 and ERT4, likely due to clay-rich or moisture-retentive layers (Onyekuru *et al*. 2018).

Engineering Implications - The results have direct implications for pipeline installation and maintenance:

Corrosion Protection: The consistently high resistivity values (>5 Ωm) eliminate the need for cathodic protection systems, reducing project costs (Figures 2–7).

Optimal Pipeline Routing: The northwestern region (Figures 8–9) is ideal for pipeline placement due to its persistently high resistivity.

Burial Depth Considerations: Deeper layers (>3 m) exhibit higher resistivity (Figures 2–7), suggesting that pipelines buried at these depths would benefit from enhanced natural protection.

Methodological Strengths and Limitations -

The reliability of these findings is reinforced by:

Standardized Schlumberger array configurations (Tables 2–7).

Comprehensive spatial coverage with six test points (Figure 1).

Integration of 1D and 3D models for robust interpretation.

However, seasonal groundwater fluctuations could influence resistivity values. Periodic monitoring is recommended to account for such variability. Future studies could also employ complementary methods (e.g., induced polarization) to further validate these results.

Conclusion

This study has successfully characterized the subsurface electrical resistivity distribution at the ELPS CS1 site in Ologbo, Edo State using the Schlumberger electrical resistivity method. The comprehensive analysis of 1D resistivity models (Figures 2-7) and 3D resistivity distribution maps (Figures 8-9) leads to the following key conclusions:

The measured resistivity values ranging from 55.2 to 9805 Ωm across all test locations and depths significantly exceed the critical 5 Ωm threshold for corrosion protection, indicating excellent natural protection for buried metallic pipelines.

The vertical resistivity profiles show a consistent pattern of high near-surface resistivity (>1000 Ωm) decreasing at intermediate depths (1-3 m) and increasing again in deeper layers (>5 m), reflecting the transition from lateritic topsoil to clay-rich intermediate layers and finally to more consolidated sandy formations.

Spatial analysis reveals optimal pipeline routing conditions in the northwestern sector of the site, where resistivity values remain consistently high (>1000 Ωm) at both surface and 5 m depth (Figures 8-9).

The uniformly high resistivity values throughout the investigated depth range (0-10 m) demonstrate that buried pipelines at this site will not require additional cathodic protection measures, resulting in significant cost savings for infrastructure development. The elimination of cathodic protection requirements could yield 23-42% cost savings in maintenance over a 20-year lifespan, as demonstrated in similar tropical environments (Uchegbulam *et al*. 2023).

These findings provide strong evidence that the ELPS CS1 site offers favorable conditions for safe pipeline installation and long-term operation. The methodology employed, combining detailed 1D vertical electrical soundings with 3D spatial analysis, has proven effective for comprehensive site characterization. Future work could investigate seasonal variations in resistivity to further validate these results (Nwankwo *et al*. 2023)

References

Akujieze, C.N. (2004). Effects of Anthropogenic Activities (Sand Quarrying and Waste Disposal) on Urban Groundwater System and Aquifer Vulnerability Assessment in Benin City, Edo State, Nigeria. *PhD Thesis, University of Benin, Benin City, Nigeria.*

Ezeh *et al*. (2023). Geoelectrical characterization of tropical lateritic soils for infrastructure development. *Journal of African Earth Sciences, 198, 104781.*

Nwajide, C.S. (2005). A guide to geological field trips to Anambra and related basins in Southeastern Nigeria. *Great AP Express Publishers Ltd.*

Nwankwo *et al*. (2023). Climate change impact on soil corrosivity in West Africa. *Scientific African, 19, e01523.*

Obrike, S.E. (2012). Evaluation of Imo clay-shale state the figure Southwestern Nigeria, as drilling mud clay. *Journal of Applied Technology of Environmental Sanitation 1 (4): 311-316.*

Obrike, S.E., Osadebe, C.C., Onyeobi, T.U.S. (2007). Mineralogical, geochemical, physical and industrial characteristics of shale from Okada area, southwestern Nigeria. *Journal Mining and Geology 43 (2): 109-116.*

Okoye, I.P., Obi, C. (2011). Synthesis and Characterization of Al- Pillared Bentonite Clay Minerals. *Research Journal of Applied Sciences 6: 447-450.*

Onyekuru, S.O., Iwuoha, P.O., Iwuagwu, C.J., Nwozor, K.K., Opara K.D. (2018). Mineralogical and geochemical properties of Clay deposits in parts of Southeastern Nigeria. *International Journal of Physical Sciences 13 (14): 217-229.*

Petters, S.W. and Ekweozor, C.M. (1981). Origin of Cretaceous black shales in the Benue Trough, Nigeria. *Journal of Palaeogeography Palaeoclimatology Palaeoecology 40: 311- 319.*

Short, K.C. and Stauble, A.J. (1967). Outline of the Geology of Onitsha, Owerri and Benue Provinces. *Geological Survey of Nigeria, Bulletin No. 21*

Uchegbulam *et al.* (2023). Geoelectrical assessment of soil aggressiveness on buried pipelines in tropical environments. *Heliyon, 9(3), e13861.*

Nwajide, C.S., (2005). A guide to geological field trips to Anambra and related basins in Southeastern Nigeria. *Great AP Express Publishers Ltd.*

Obrike, S.E., (2012). Evaluation of Imo clay-shale deposit (Paleocene) from Okada, Edo State, Southwestern Nigeria, as drilling mud clay. *Journal of Applied Technology of Environmental Sanitation 1 (4), 311-316.*

Obrike, S.E., Osadebe, C.C., Onyeobi, T.U.S., (2007). Mineralogical, geochemical, physical and industrial characteristics of shale from Okada area, southwestern Nigeria. *Journal Mining and Geology 43 (2), 109-116.*

Okoye, I.P., Obi, C., (2011). Synthesis and Characterization of Al- Pillared Bentonite Clay Minerals. *Research Journal of Applied Sciences 6, 447-450.*

Onyekuru, S.O., Iwuoha, P.O., Iwuagwu, C.J., Nwozor, K.K., Opara K.D., (2018). Mineralogical and geochemical properties of Clay deposits in parts of Southeastern. *Nigeria. International Journal of Physical Sciences 13 (14), 217-229.*

Petters, S.W., Ekweozor, C.M., (1981). Origin of Cretaceous black shales in the Benue Trough, Nigeria. *Journal of Palaeogeography Palaeoclimatology Palaeoecology 40, 311- 319.*

Reyment, R.A., 1965. Aspects of the Geology of Nigeria. *Ibadan University Press, Ibadan.*

Short, K.C., Stauble, A.J., (1967). Outline of the Geology of Onitsha, Owerri and Benue Provinces. *Geological Survey of Nigeria, Bulletin No. 21*